Three-dimensional measurement using tomography systems in a magnetized plasma in linear cylindrical geometry

K. Yamasaki[1], A. Fujisawa[2,3], Y. Nagashima[2,3], C. Moon[2,3], S. Inagaki[2,3], M. Sasaki[5], Y. Kosuga[2,3], T. Yamada[3,4], N. Kasuya[2,3]

[1] *Graduate School of Advanced Science and Engineering, Hiroshima University, Hiroshima, Japan*

[2] *Research Institute for Applied Mechanics, Kyushu University, Kasuga, Fukuoka, Japan*

[3] *Research Center for Plasma Turbulence, Kyushu University, Kasuga, Fukuoka, Japan*

[4] *Faculty of Arts and Science, Kyushu University, Fukuoka, Fukuoka, Japan*

[5] *College of Industrial Technology, Nihon University, Chiba, Japan*

Introduction

Fluctuations play a crucial role in heat and particle transport in magnetized plasmas. Recent theoretical and experimental studies have suggested that multiscale interaction between small- and large-scale fluctuations is an essential element for transport, especially for nonlocal transport in magnetized plasma [1, 2]. Therefore, in order to elucidate mechanism of nonlocality induced by such nonlinear interaction of fluctuations, a new diagnostic system is required to observe the entire region of plasma with high spatial and temporal resolution. For this purpose, we have developed tomography systems to observe a whole cross section of a linear cylindrical plasma produced in a device named PANTA (Plasma Assembly for Nonlinear Turbulence Analysis) [3]. Recently, three tomography systems have been installed in PANTA, and finally developed to be able to observe three-dimensional (3D) structure of plasma emission and its fluctuations [4].

Although we can obtain fluctuation data over the whole cross section of PANTA plasma by using the tomography systems, a specialized analysis method is required for extracting useful information from temporal series of three tomography systems. For example, we need a method to transform 2D plasma profile, initially reconstructed on a cartesian coordinate, to a cylindrical one for simple analyses. For this purpose, we have invented so-called Fourier-Rectangular Function (FRF) analysis to express the cartesian tomography data on a cylindrical coordinate. In this presentation, we introduce the 3D tomography measurement recently achieved in PANTA and present the obtained results from the combination of the 3D tomography measurement and the FRF analysis.

Three tomography systems

The PANTA device in which the tomography systems are installed can produce cylindrical-shaped magnetized Ar plasmas with 4.0 m in length and 10 cm in diameter using 7 MHz RF[3]. The three systems of tomography are categorized to two kinds; one is composed of four sets of light guide arrays placed on a vacuum chamber, spaced by 45 degrees apart in the azimuthal direction (called TS-A), while the other is composed of six sets of light guide arrays placed by 30 degrees apart (TS-B) (see Fig. 1). The light guide arrays of TS-A and TS-B comprise 32 and 21 stainless collimators, respectively, which limit the viewing angle, spaced 5 mm apart [5], [6]. The plasma images are reconstructed on squared regions of 16 cm x 16 cm and 10 cm × 10 cm in TS-A and TS-B, respectively, as 11 x 11 grid image using the algorithm of Maximum Likelihood-Expectation Maximization (MLEM) method [7], as shown in Figs 2(a) and 2(b). The fluctuation of local emission can be observed with a sufficiently high signal-to-noise ratio. Using these three tomography systems, we have successfully observed 3D structure of fluctuations in magnetized plasma as shown in Fig. 2(c).

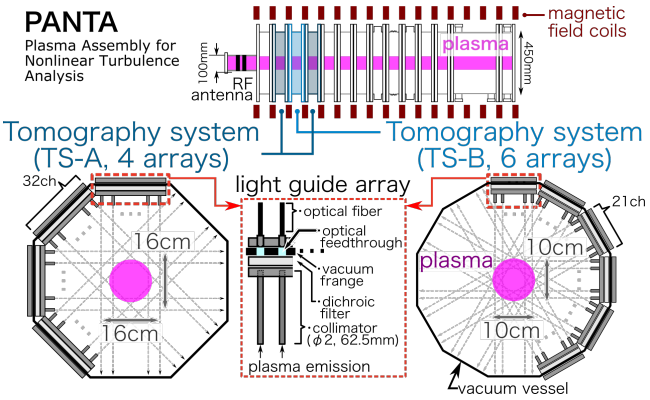

Figure 1 Schematic view of PANTA and tomography systems.

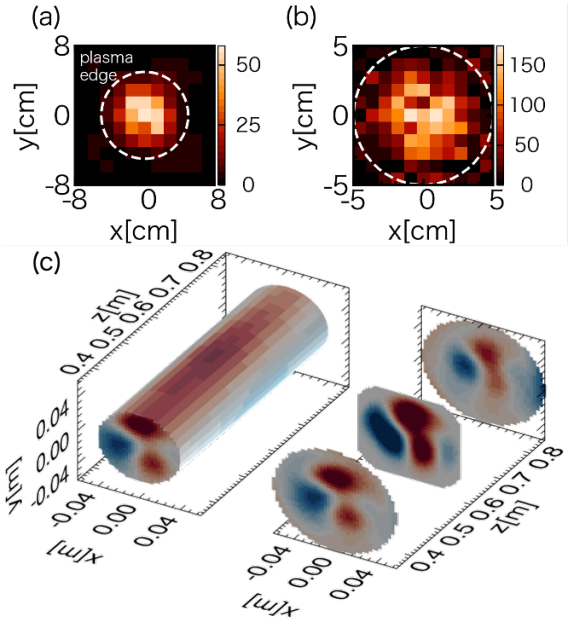

Figure 2 (a)(b) MLEM reconstuction images of TS-A and TS-B, respectively. (c) An example of 3D structure of fluctuation obtained by the three tomography systems.

Fourier-Rectangular Function Analysis

The Fourier-Rectangular Function (FRF) expansion is developed to analyze the 2D image data on a Cartesian coordinate as that on a cylindrical one. A two-dimensional image in cylindrical coordinates (r, θ) is expanded in a combined form of rectangular and sinusoidal function series, $\phi_i(r,\theta)$,

$$\varepsilon(r,\theta) = \sum_{i=1}^{Nr} a_{i,0}\frac{R_i(r)}{\sqrt{2}} + \sum_{i=1}^{Nr}\sum_{m=1}^{M} R_i(r)\left[a_{i,m}^{c}\cos m\theta + a_{i,m}^{s}\sin m\theta\right] = \sum_{l=1}^{L} a_l\phi_l(r,\theta),$$

where $R_i(r)$ is a rectangular function. In the final reduction of above equation, the correspondence of bases is that $\phi_l(r,\theta) = R_n(r)/\sqrt{2}(l=i)$, $\phi_l(r,\theta) = R_i(r)\cos m\theta$ $(l = 2N_r(m-1)+N_r+i, m>0)$, $\phi_l(r,\theta) = R_i(r)\sin m\theta$ $(l = 2N_r(m-1)+N_r+i+1, m>0)$. Then, the base functions satisfy the following quasiorthonormal relationships:

$$\int_0^a \int_0^{2\pi} \phi_i(r,\theta)\phi_j(r,\theta) r dr d\theta = \delta_{i,j},$$

where $\delta_{i,j}$ represents the Kronecker's delta. Using the orthonormal relationship, one can obtain the coefficient of each basis function, $a_{0,n}, a^c_{m,n}, a^s_{m,n}$, as follows,

$$a_{i,0} = \int \varepsilon(r,\theta)\frac{R_i(r)}{\sqrt{2}} r dr d\theta,$$

$$a^c_{i,m} = \int \varepsilon(r,\theta) R_i(r)\cos m\theta\, r dr d\theta,$$

$$a^s_{i,m} = \int \varepsilon(r,\theta) R_i(r)\sin m\theta\, r dr d\theta.$$

Obtaining the time series data of these coefficients, $a_{i,0}(t), a^c_{i,m}(t), a^s_{i,m}(t)$, analysis is performed on the complex coefficient $c(r_i,m,t) = a^c_{i,m}(t) + \sqrt{-1}a^s_{i,m}(t)$ to obtain the feature of the spatio-temporal structure of fluctuation.

Application of FRF Analysis and 3D Measurement

Figure 3 shows an example of the FRF analysis on a PANTA plasma under the following operation condition: magnetic field strength of 1300 G, filling Ar gas pressure of 3 mTorr, and RF input power of 6 kW. The power spectrum of local emission intensity at r = 1.8 cm (x = 1.8 cm, y = 0.0 cm) is shown, for example, in Fig. 3(a). In this case, coherent fluctuations are observed at 2 kHz, 7 kHz, 9 kHz and 11kHz. By calculating Fourier spectrum of the complex coefficient of FRF $c_z(r_i,m,t)$, denoted as $\hat{c}_z(r_i,m,f)$, one can obtain the power spectrum as a function of the azimuthal mode number and frequency, *i.e.*, dispersion relationship, at each radial location, $P(r_i,m,f) = |\hat{c}_z(r_i,m,f)|^2$, where z means the axial position a tomography system observes. Figure 4(a) shows the dispersion relationship, which indicates that the coherent fluctuations at 2, 7, 9 and 11 kHz have azimuthal mode number of 1, 3, 4 and 5, respectively. The spatial structure of the coherent fluctuations are evaluated using the power $P(r_i,m,f)$ and

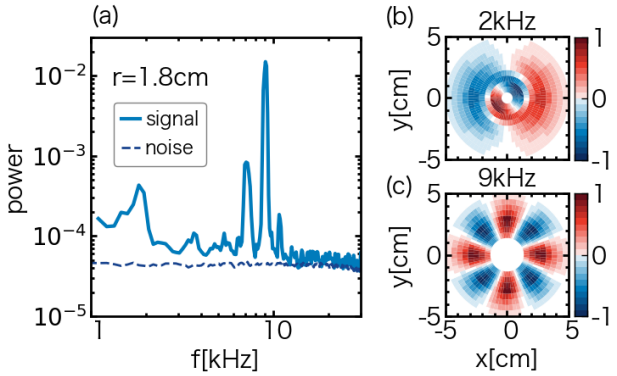

Figure 3 (a) A power spectrum of local emission intensity at r = 1.8 cm. (b) and (c) Spatial structures of coherent modes of 2 kHz and 9 kHz, respectively.

the cross-phase to the reference radial location (r_{ref}), $\Theta(r_i, m, f) = \mathrm{Arg}[\hat{c}_z(r_i, m, f)\hat{c}_z^*(r_{ref}, m, f)]$, as follows,

$$\bar{\varepsilon}(r, \theta, m, f) = \sqrt{P(r_i, m, f)}\cos(m\theta + \Theta(r_i, m, f)),$$

where $\hat{c}_z^*(r_i, m, f)$ is the conjugate of $\hat{c}_z(r_i, m, f)$. The examples of the reconstructed structure are shown for the modes of (m, f) = (1, 2 kHz) and (4, 9 kHz) in Figs. 3(b) and 3(c).

Also, the complex coefficients of the FRF expansion can be used to calculate the radial and axial wavenumber. Taking the two-dimensional histogram of the following two values,

$$k_r = \frac{\mathrm{Arg}[\hat{c}_z(r_i, m, f)\ \hat{c}_z^*(r_{i-1}, m, f)]}{\Delta r}, k_z = \frac{\mathrm{Arg}[\hat{c}_{z+\Delta z}\ (r_i, m, f)\hat{c}_z^*(r_i, m, f)]}{\Delta z},$$

one can obtain the kz - kr spectrum. Figure 4 (b) and 4(c) shows the kz – kr spectrum of m=1 and 4 modes, respectively. Since it is difficult to distinguish such a 3D structure for each frequency with 1D measurement system or local imaging technique, for example, with reflectometry, GPI and BES, the tomography systems should have the prominent feature to be able to obtain dispersion relation and 3D wavenumber spectrum at every radial location using the FRF analysis. The obtained 3D wavenumbers could contribute to investigate the fluctuations, such as their driving mechanisms [9,10].

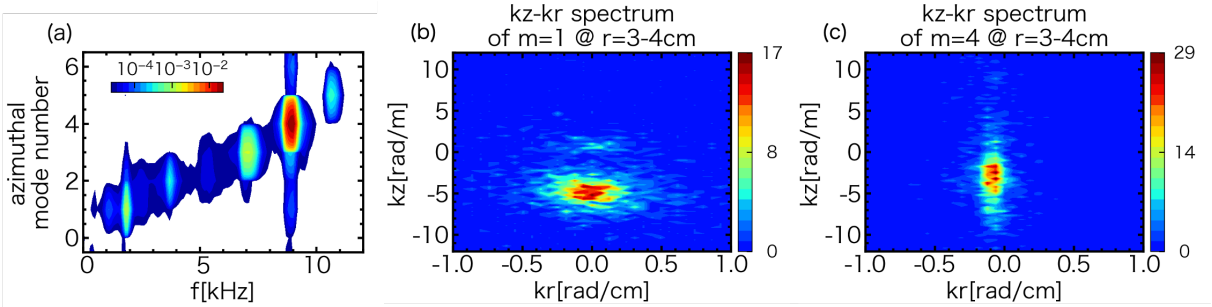

Figure 4 (a) Azimuthal mode number-frequency spectrum at r = 4 cm. (b) and (c) The kz - kr spectrum of m=1 and m=4 mode, respectively.

To summarize, the combination of the whole cross section observation and the FRF analysis gives us access to the advanced analysis on turbulence in magnetized plasmas.

This work is supported by JSPS KAKENHI Grant Numbers JP17H06089, 17K06994, 15H02335, 19K23426, and 20K14443, and also by NIFS Collaboration Research pro- gram NIFS17KOCH002.

References

[1] K. Ida *et al*., Nucl. Fusion, **55** (2015) [2] J. D. Callen and M. W. Kissick, Plasma Phys. Control. Fusion, **39** (1997) [3] S. Oldenbürger *et al*., Plasma Phys. Control. Fusion, **54** (2012) [4] C. Moon, K. Yamasaki *et al*., Sci. Rep., **11** (2021) [5] A. Fujisawa, et al., Plasma Phys. Control. Fusion, **58** (2016) [6] K. Yamasaki, et al., Rev. Sci. Instrum., **91** (2020) [7] L. A. Shepp and Y. Vardi, IEEE Trans. Med. Imaging, **1** (1982) [8] K. Yamasaki *et al*., J. Appl. Phys., **126** (2019) [9] Y. Kosuga, S.-I. I. Itoh, and K. Itoh, Plasma Fusion Res., **10** (2015) [10] M. SASAKI *et al*., Plasma Fusion Res., **12** (2017)